

**Supplemental Information for**

**Cannabinoid CB<sub>1</sub> receptor gene inactivation in oligodendrocyte precursors  
disrupts oligodendrogenesis and myelination in mice**

Aníbal Sánchez-de la Torre, Tania Aguado, Alba Huerga-Gómez, Silvia Santamaría, Antonietta Gentile, Juan Carlos Chara, Carlos Matute, Krisztina Monory, Susana Mato, Manuel Guzmán, Beat Lutz, Ismael Galve-Roperh & Javier Palazuelos

Corresponding author: Javier Palazuelos

Email: [j.palazuelos@ucm.es](mailto:j.palazuelos@ucm.es)

**This PDF file includes:**

Supplementary Figures S1 to S6

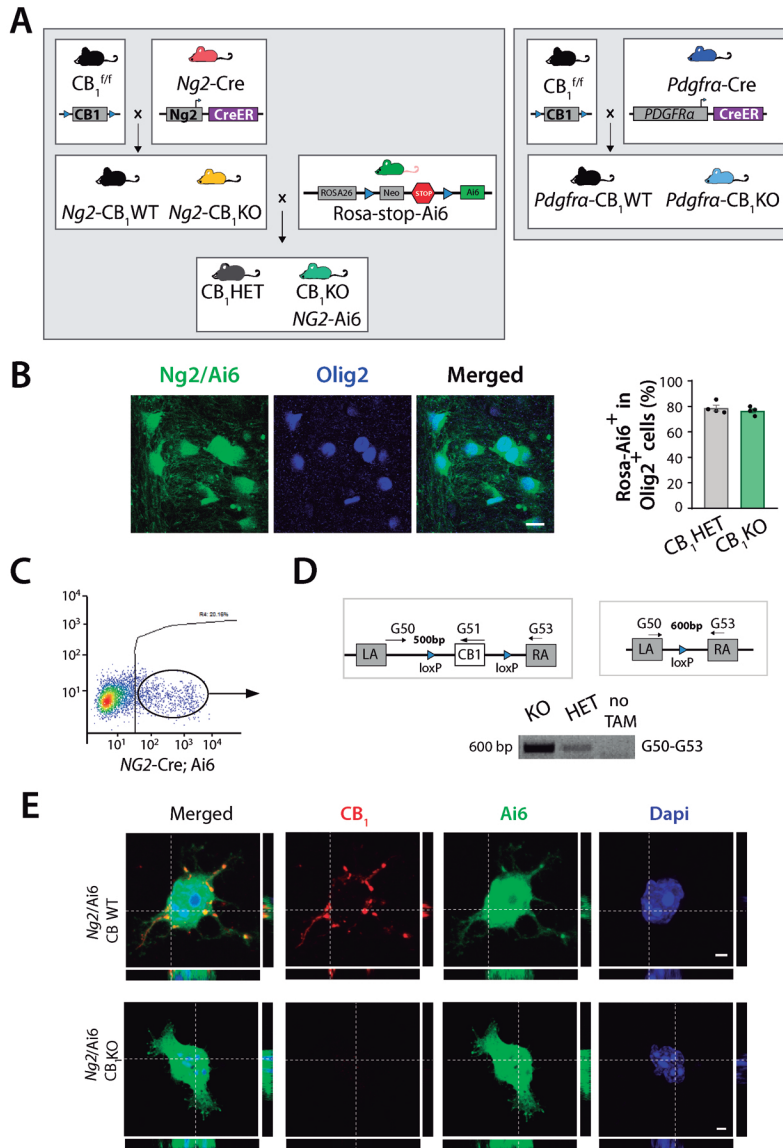


Fig. S1

**Fig. S1. Selective *CB<sub>1</sub>* receptor gene inactivation in oligodendrocyte precursor cells *in vivo*.** **A** Diagram of the generation of the *Ng2/Ai6-CB<sub>1</sub>KO* and *Pdgfra-CB<sub>1</sub>KO* mouse lines. **B** Recombination efficiency was determined by immunofluorescence analysis in the *corpus callosum* at postnatal day 11, following tamoxifen-driven recombination at postnatal day 6 (P6, P7). Representative images and quantification of the percentage of *Rosa-Ai6<sup>+</sup>* cells among *Olig2<sup>+</sup>* cells. **C** Representative image of FAC-sorting analysis of *Ng2/Ai6-CB<sub>1</sub>KO* and control *Ng2/Ai6-CB<sub>1</sub>HET* cells. **D** Genetic recombination of the *CB<sub>1</sub>* locus in the *Ai6<sup>+</sup>* cell population was confirmed by genomic DNA extraction of FAC-sorted *Ng2/Ai6-CB<sub>1</sub>KO* and control cells. **E** Immunofluorescence analysis of *CB<sub>1</sub>* receptors in *Ng2/Ai6-CB<sub>1</sub>WT* and *Ng2/Ai6-CB<sub>1</sub>KO* cells obtained from the CC and attached to glass slides. Representative confocal images showing orthogonal plane. Data are shown as mean  $\pm$  SEM.  $n = 4$  for **B** independent data points used per experimental group. Scale bars, 20  $\mu$ m.

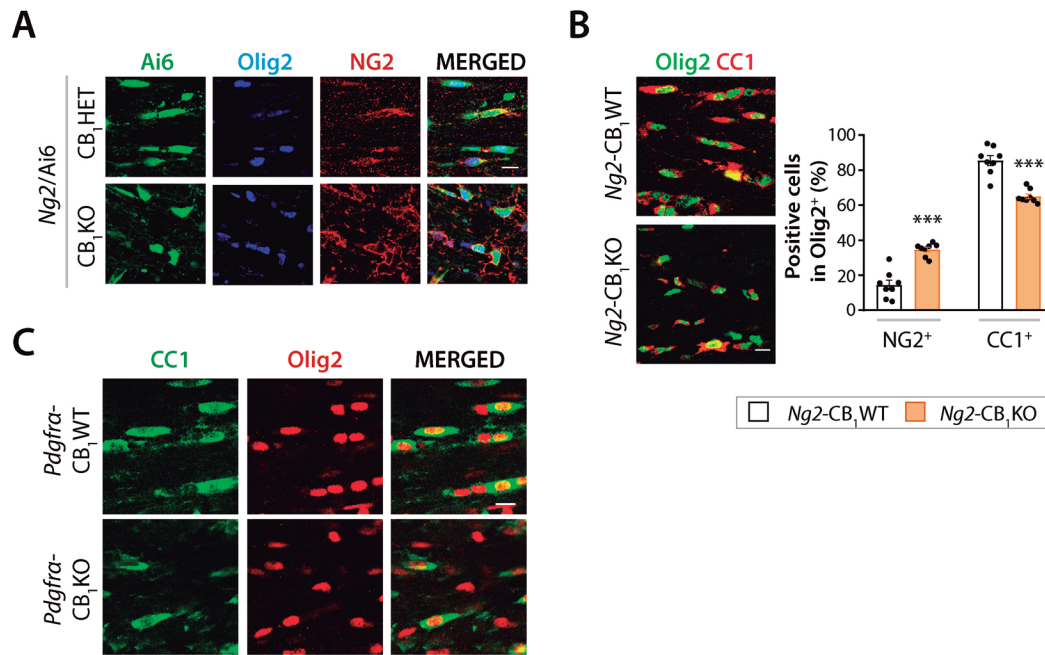


Fig. S2

**Fig. S2. CB<sub>1</sub> receptor gene inactivation in OPC blocks cell differentiation.**

Tamoxifen-driven recombination was induced at postnatal day 6 (P6-P7) in *Ng2/Ai6*-CB<sub>1</sub>HET and *Ng2/Ai6*-CB<sub>1</sub>KO mice (A), *Ng2*-CB<sub>1</sub>KO (B), or *Pdgfra*-CB<sub>1</sub>KO and control mice (C), and oligodendrogenesis was analyzed in the *corpus callosum* at P15 (A and C) and P60 (B). Representative confocal microscopy in the *corpus callosum* immunostained with the indicated antibodies (A and C). B Immunofluorescence analysis and quantification of the percentage of NG2<sup>+</sup> OPCs or CC1<sup>+</sup> OLs among Olig2<sup>+</sup> cells in *Ng2*-CB<sub>1</sub>KO and *Ng2*-CB<sub>1</sub>WT mice at P60. Data are shown as mean +/- SEM. n = 8 for B, independent data points used per experimental group, \*\*\*p ≤ 0.001 vs *Ng2*-CB<sub>1</sub>WT mice by two-tailed unpaired Student's t-test. Scale bars, 20 μm.

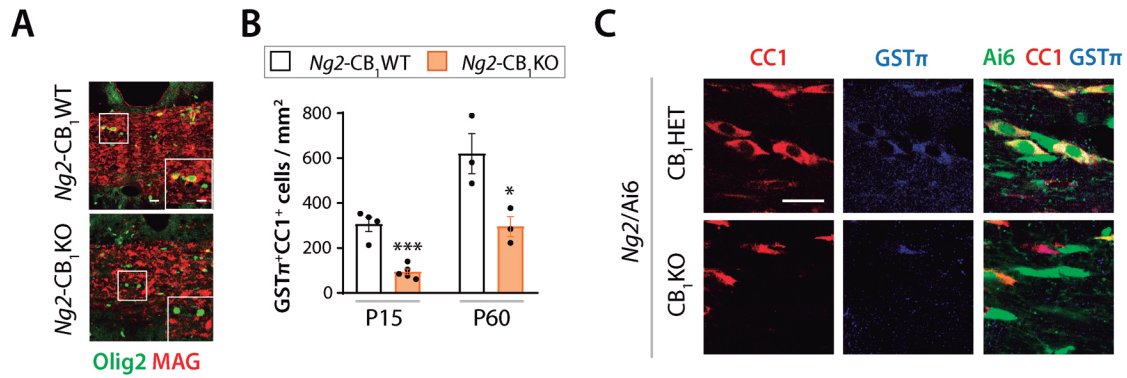


Fig. S3

**Fig. S3. CB<sub>1</sub> receptor gene inactivation in OPC disrupts oligodendrocyte maturation.** Tamoxifen-driven recombination was induced at postnatal day 6 (P6-P7) in *Ng2-CB<sub>1</sub>KO* and *Ng2-CB<sub>1</sub>WT* mice (**A** and **B**), or *Ng2/Ai6-CB<sub>1</sub>KO* and *Ng2/Ai6-CB<sub>1</sub>HET* mice (**C**) mice, and oligodendrocyte maturation was analyzed in the *corpus callosum* (CC) at P15 (**B** and **C**) and P60 (**A** and **B**). **A** Representative confocal microscopy images in the CC immunostained with MAG and Olig2 antibodies. **B** Immunofluorescence analysis and quantification of the density of GST $\pi$ <sup>+</sup>CC1<sup>+</sup> mature OLs. **C** Representative confocal images of indicated antibodies. Data are shown as mean  $\pm$  SEM. n = 3-5 for **B**, independent data points used per experimental group, \*p  $\leq$  0.05, \*\*p  $\leq$  0.01 vs *Ng2-CB<sub>1</sub>WT* mice by two-tailed unpaired Student's t-test. Scale bars, 20  $\mu$ m for **A** and **C**, 10  $\mu$ m for inset in **A**.

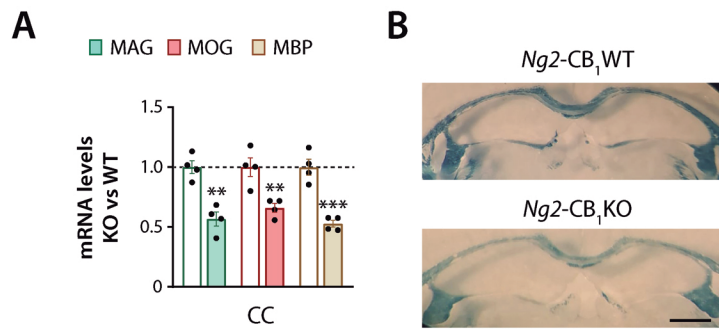


Fig. S4

**Fig. S4. CB<sub>1</sub> receptor gene inactivation in OPCs causes hypomyelination in young adult mice.** Tamoxifen-driven recombination was induced at postnatal day 6 (P6-P7) in *Ng2-CB<sub>1</sub>KO* and *Ng2-CB<sub>1</sub>WT* mice and myelination was analyzed at P60. **A** qPCR analysis of myelin-associated mRNA levels in the CC at P60. **B** Sudan Black staining at the caudal CC. Data are shown as mean +/- SEM. n = 4 for **A**, independent data points used per experimental group, \*\*p ≤ 0.01, \*\*\*p ≤ 0.001 vs *Ng2-CB<sub>1</sub>WT* mice by two-tailed unpaired Student's t-test. Scale bars 600 μm for **B**.

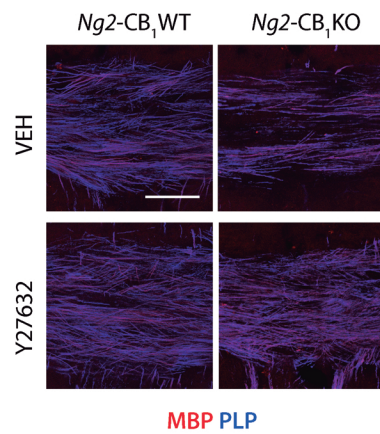


Fig. S5

**Fig. S5. Pharmacological ROCK inactivation overcomes the defects in developmental myelination of CB<sub>1</sub> deficient OPCs at postnatal ages.** Tamoxifen-driven recombination was induced at postnatal day 6 (P6-P7) in *NG2-CB<sub>1</sub>KO* and *NG2-CB<sub>1</sub>WT* mice followed by administrations of the ROCK inhibitor Y-27632 (10 mg/kg), and tissue was analyzed at P11. Representative images of immunofluorescence analysis for the myelin-associated proteins proteolipid protein (PLP) and myelin basic protein (MBP). Scale bar, 80  $\mu$ m.

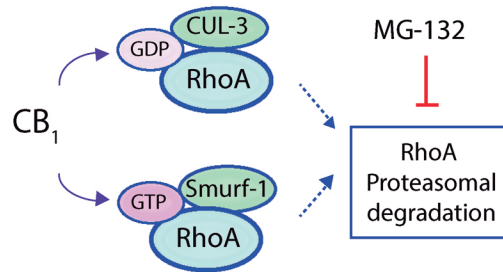


Fig. S6

**Fig. S6. Diagram representing the proposed model of CB1 receptor modulation of RhoA proteasomal degradation.** CB1 receptor, by inducing Smurf-1/CUL-3 mediated RhoA proteasomal degradation, modulates OPC differentiation.